MTGAN: Mask and Texture-driven Generative Adversarial Network for Lung Nodule Segmentation

Wei Chen (wchen@cqu.edu.cn)

Backgrounds

Backgrounds

Lung Nodule Segmentation

- Lung cancer is one of the most frequently diagnosed cancers in the world, approximately 70% of which are diagnosed at advanced stages.
- Accurate segmentation for lung nodules in lung computed tomography (CT) scans plays a key role in the early diagnosis of lung cancer.
- However, due to the complex shapes of lung nodules and the similarity of visual characteristics between nodules and lung tissues, an accurate segmentation with low false positives of lung nodules is still a challenging problem.

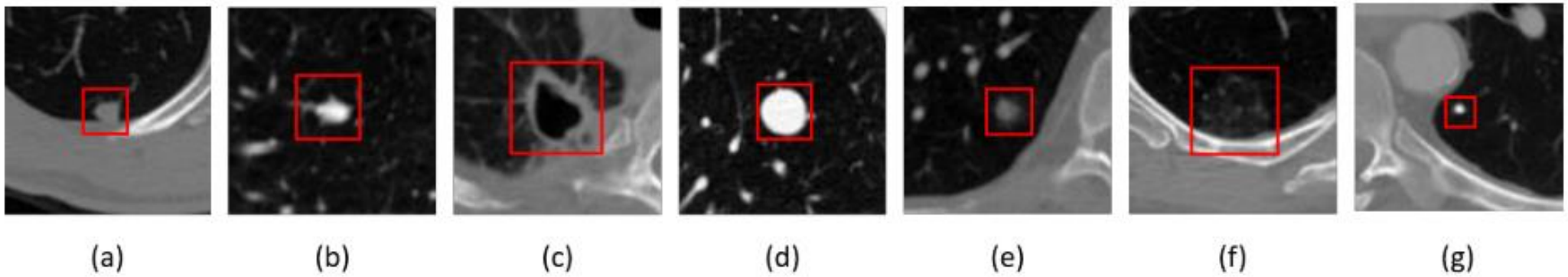

Fig. 1. Example images of seven typical lung nodules in CT scans: (a) juxtapleural nodule, (b) isolated nodule, (c) cavitary nodule, (d) calcified nodule, (e) mixed ground-glass nodule, (f) pure ground-glass nodule, (g) small nodule having a diameter of less than 5 mm.

Backgrounds

GAN-based methods for medical image segmentation.

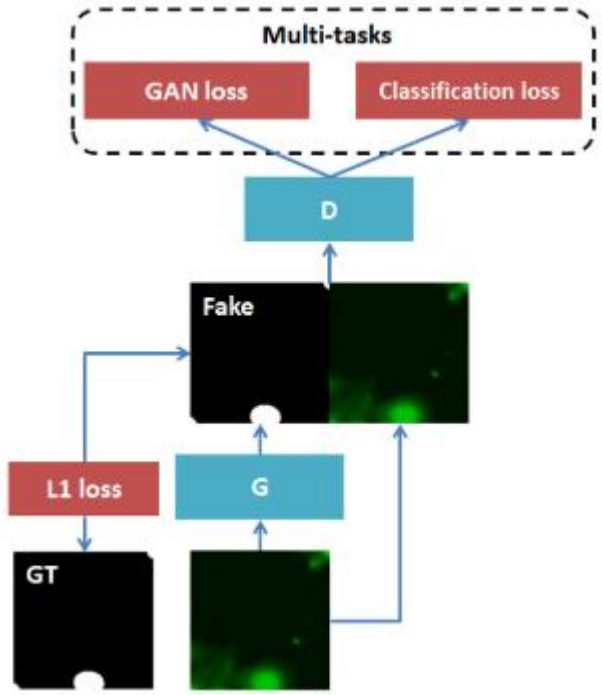

Y. Li and L. Shen, "cc-gan: A robust transfer-learning framework for hep-2 specimen image segmentation," IEEE Access, vol. 6, pp. 14 048– 14 058, 2018.

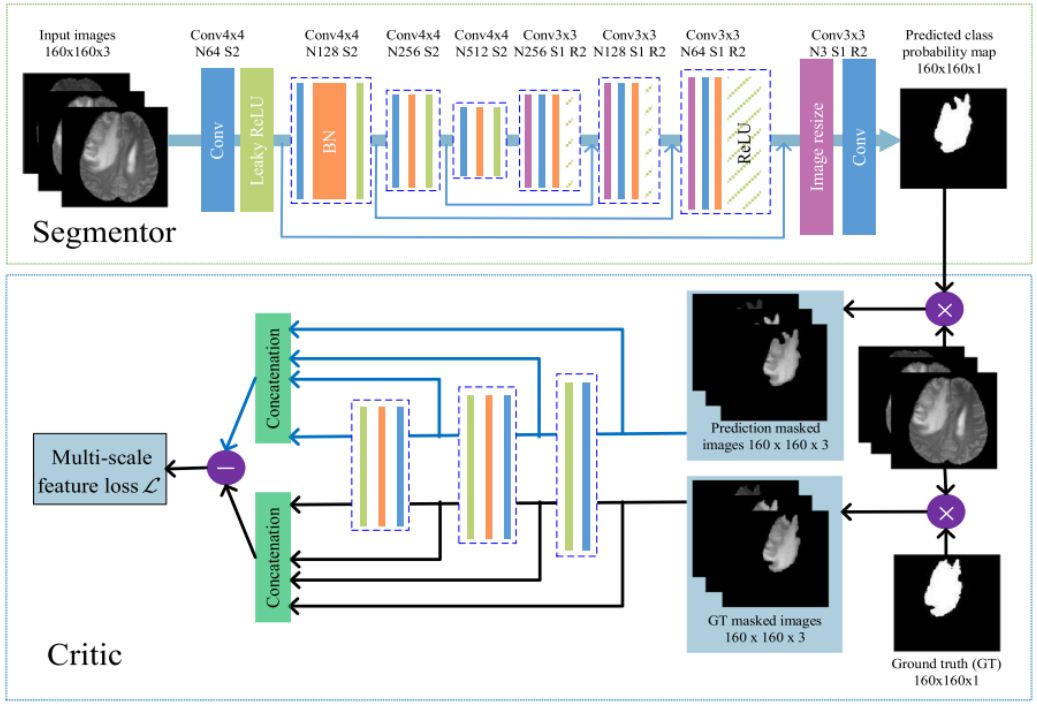

Y. Xue, T. Xu, H. Zhang, L. R. Long, and X. Huang, "Segan: Adversarial network with multi-scale l 1 loss for medical image segmentation," Neuroinformatics, vol. 16, no. 3-4, pp. 383–392, 2018.

MTGAN: Mask and Texture-driven Generative Adversarial Network for Lung Nodule Segmentation

MTGAN

Architecture And Loss

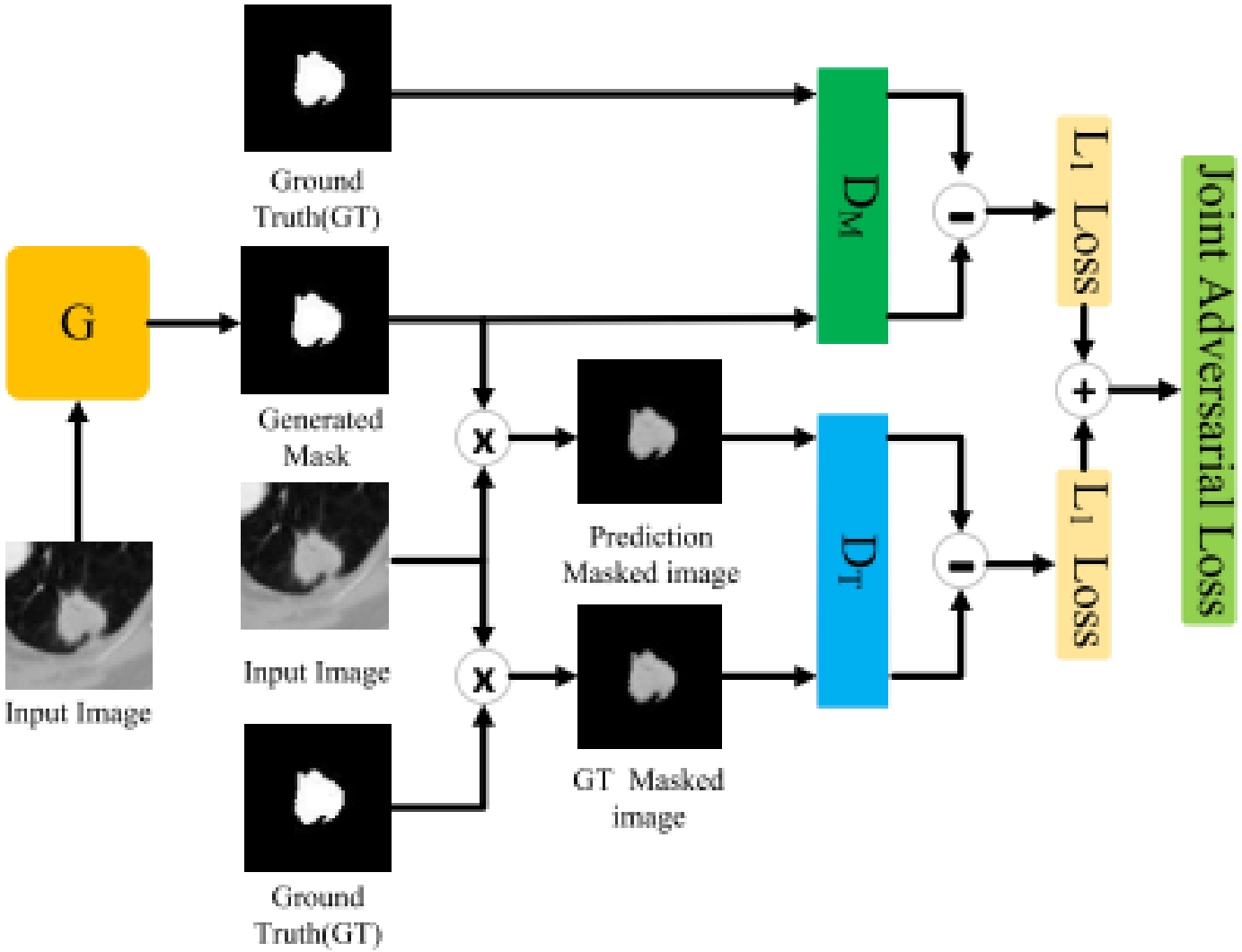

$$L_{D_M} = \frac{1}{N}\sum_{i=1}^{N} \left\| D_M^i(Y_{pre}) - D_M^i(Y_{gt}) \right\|_1 \quad (1)$$

$$L_{D_T} = \frac{1}{N}\sum_{i=1}^{i=N} \left\| D_T^i(X \cdot Y_{pre}) - D_T^i(X \cdot Y_{gt}) \right\|_1 \quad (2)$$

$$L_G = L_{D_M} + L_{D_T} \quad (3)$$

$$obj = \arg\min_{G}(L_G(\arg\max_{D_M, D_T}(L_{D_M}, L_{D_T}))) \quad (4)$$

Experiments

Experiments

Lung Nodule Segmentation

TABLE I

COMPARISON WITH DIFFERENT TRAINING STRATEGIES. EACH TABLE CELL SHOWS MEAN ± SD.

Model	DSC%	IoU%
G (Modified U-Net)	84.93 ± 9.05	74.74 ± 12.13
$G + D_M$	84.96 ± 9.50	74.85 ± 12.86
$G + D_T$	85.12 ± 9.12	75.07 ± 12.37
$G + D_M + D_T$	**85.24 ± 9.01**	**75.22 ± 12.26**

Experiments

Lung Nodule Segmentation

TABLE II
COMPARISON THE RESULTS OF OUR MTGAN (HIGHLIGHTED IN BOLD) AGAINST OTHER METHODS FOUND IN THE LITERATURE.

Method	DSC%	IoU%
Level Set [37]	60.63 ± 17.39	-
Graph Cut [37]	68.90 ± 16.03	-
CF-CNN [37]	82.15 ± 10.76	-
Dual-branch Resnet [38]	82.74	-
U-Net (Multi-orientation) [16]	83.00	76.00
NoduleNet [39]	83.10 ± 8.85	71.85 ± 10.48
Priori-based U-Net [36]	85.86 ± 1.24	-
MTGAN	**85.24 ± 9.01**	**75.22 ± 12.26**

Experiments

Lung Nodule Segmentation

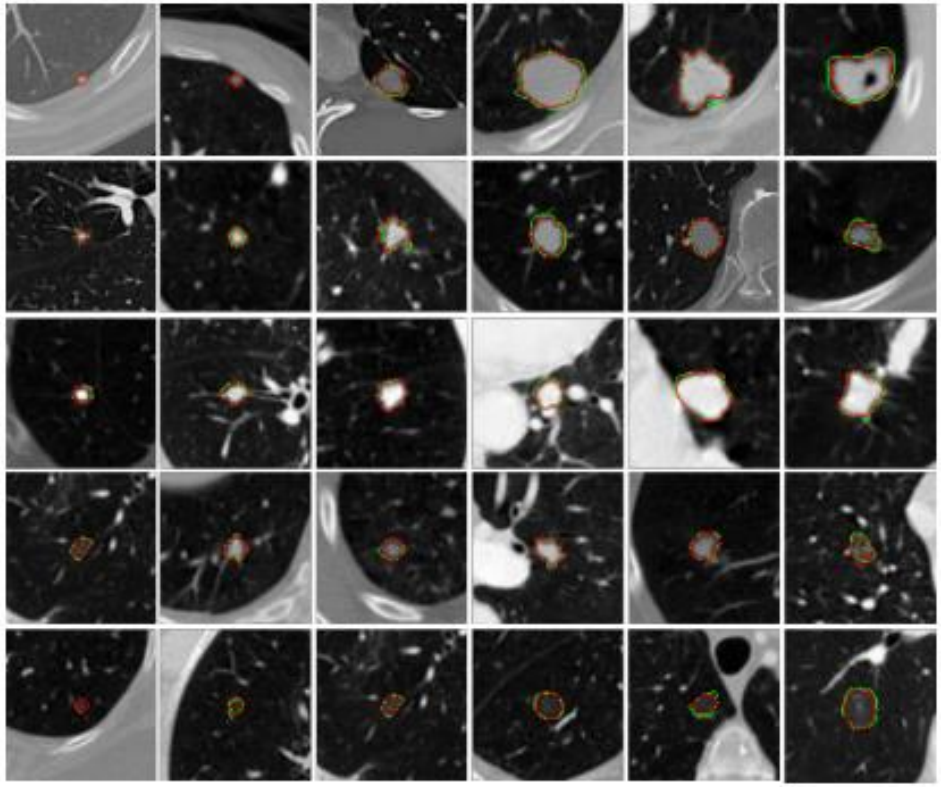

Segmentation results of the proposed MTGAN. From top to bottom: juxtapleural nodules, isolated nodules, calcified nodules, mixed ground-glass nodules, pure ground-glass nodules. The red contours represent segmentation results generated by MTGAN, and the green contours are ground truth.

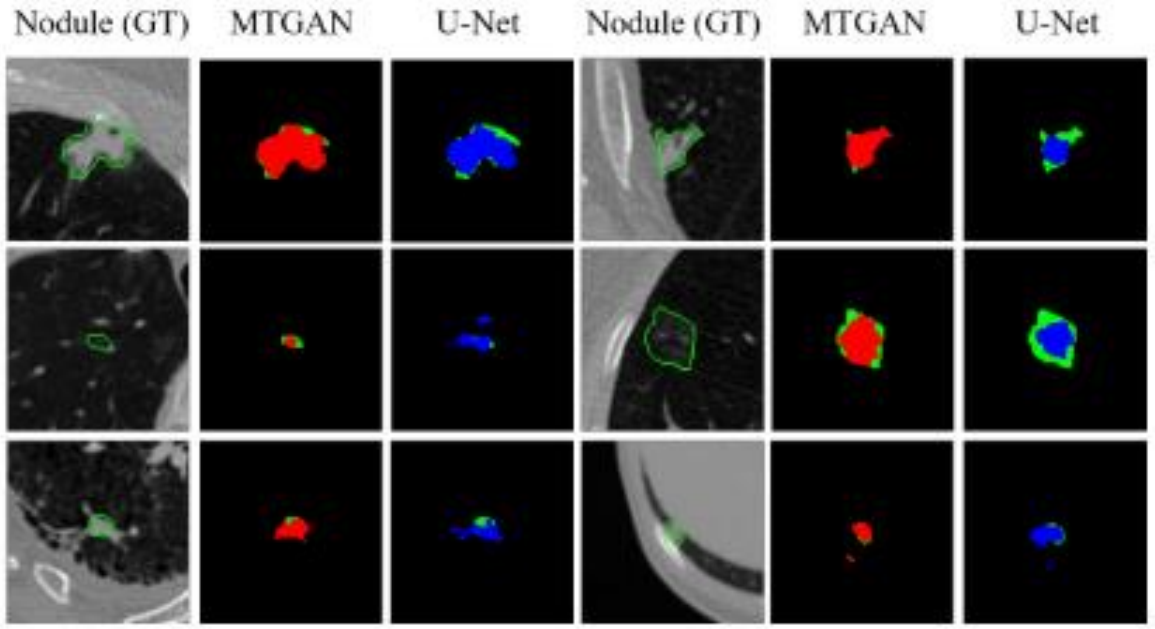

Visualized segmentation results of the proposed MTGAN (red color) and U-Net (blue color). The first row shows the segmentation results of juxtapleural nodules, and the second row is the segmentation results of low-dense nodules. The last row indicates that our method can effectively reduce the false positive rate.

THANKS